

See discussions, stats, and author profiles for this publication at: <https://www.researchgate.net/publication/231705892>

Silyl Radical Chemistry and Conventional Photoinitiators: A Route for the Design of Efficient Systems

ARTICLE *in* MACROMOLECULES · AUGUST 2009

Impact Factor: 5.8 · DOI: 10.1021/ma901003h

CITATIONS

21

READS

59

8 AUTHORS, INCLUDING:



Jacques Lalevée

Université de Haute-Alsace

338 PUBLICATIONS 4,056 CITATIONS

SEE PROFILE



Anne-Caroline Chany

University of Oxford

13 PUBLICATIONS 108 CITATIONS

SEE PROFILE



Mohamad El-Roz

French National Centre for Scientific Research

44 PUBLICATIONS 664 CITATIONS

SEE PROFILE



Xavier Allonas

Université de Haute-Alsace

206 PUBLICATIONS 2,919 CITATIONS

SEE PROFILE

Silyl Radical Chemistry and Conventional Photoinitiators: A Route for the Design of Efficient Systems

J. Lalevée,^{*,†} N. Blanchard,[‡] A. C. Chany,[‡] M. El-Roz,[†] R. Souane,[†] B. Graff,[†] X. Allonas,[†] and J. P. Fouassier[†]

[†]Department of Photochemistry, CNRS, University of Haute Alsace, ENSCMu, 3 rue Alfred Werner, 68093 Mulhouse Cedex, France, and [‡]Department of Organic and Bioorganic Chemistry, CNRS, University of Haute Alsace, ENSCMu, 3 rue Alfred Werner, 68093 Mulhouse Cedex, France

Received May 8, 2009; Revised Manuscript Received June 17, 2009

ABSTRACT: Three new efficient photoinitiators (PI) based on a well-known chromophore skeleton (hydroxyphenylacetophenone, thioxanthone, or benzoin) linked to a silyl-containing moiety are proposed. The ability of these structures to initiate both free radical polymerization and free radical promoted cationic polymerization is investigated. A comparison with parent compounds is provided. High rates of polymerization and high final conversions are obtained. These PI directly generate silyl radicals under light irradiation as characterized by ESR spin-trapping. The analysis of the excited-state processes through laser flash photolysis and quantum molecular calculations allow to explain the observed photochemical behavior. The present results evidence the high potential of these new modified PI.

Introduction

The development of new photoinitiators PI of radical and cationic polymerization usable in specific applications still remains very important.¹ In the recent years, attempts have been made to design new radical PIs. For example, systems involving a structural modification of existing skeletons (based on the benzoyl chromophore, benzophenone, thioxanthone, etc.) are currently designed (see e.g. refs 2–5). New type I photoinitiating systems leading to less usual radicals such as the silyl (Si[•]) or germyl (Ge[•]) radicals have been proposed^{6,7} and a lot of new type II photoinitiating systems generating silyl, thiyl (S[•]), or germyl radicals explored.^{8–10} Among these radicals, Si[•] appears promising.

The photodegradation of polysilane polymers or oligomers that occurs from a Si–Si cleavage and generates silyl radicals has been reported a long time ago.^{6a–d} The photoinitiation ability of these silyl radicals was low, but other polysilane structures exhibiting higher photoinitiation efficiencies were further proposed.^{6a–d} In the past few years, we designed new structures, based e.g. on a Si–Si, C–Si, S–Si, or Si–H bonds, leading to Si[•] radicals: the high reactivity of Si[•] toward the addition process to acrylate double bonds as well as their good behavior in photoinitiation of free radical polymerization FRP and free radical promoted cationic polymerizations FRPCP under air were outlined.⁸

The goal of the present paper is to check (i) the introduction of a silyl moiety into a usual structure of radical photoinitiator in order to generate silyl radicals and (ii) the effect on the excited state reactivity and the polymerization ability. Three starting structures largely used in the photopolymerization area (2-hydroxy-2-methyl-1-phenylpropanone (HMPP), thioxanthone, and benzoin derivatives) have been selected as shown in Scheme 1 for the design of the new proposed photoinitiators **PI-1–PI-3**.

Modification of hydroxyalkylphenyl ketone (HAP) (e.g., change of the phenyl ring or the chromophore, introduction of functional groups),^{2c,f,g} thioxanthone derivative (TX) (e.g., introduction of

new substituents to improve the properties),^{3,4a,d,e,g} and benzoin derivative (BZ) (with various functional groups)^{5a} have been already achieved: in most cases, the modified HAP, TX, and BZ behave as the parent molecules and do not generate new radicals. Some structures combining well-known PI (e.g., a modified HAP) substituted by a silane moiety have also been proposed to improve the solubility in silicone media,¹¹ but no generation of the silyl radicals has been reported as the silane substituent exhibits no interaction with the chromophore. In the same way, a benzoin trimethylsilyl ether (having a O–Si(CH₃)₃ group instead of the usual OH) has been proposed to check some substitution effect in the BZ series: no silyl radicals were reported.^{5a} The approach developed here is different, the initiation mechanism having to be strongly affected by the substitution through the generation of new initiating Si[•] radicals.

The polymerization ability of **PI-1–PI-3** in FRP and FRPCP under air will be evaluated and the silyl radical formation investigated by laser flash photolysis (LFP) and electron spin resonance spin trapping (ESR-ST) experiments. A comparison with reference photoinitiators (HMPP, 2-isopropylthioxanthone (ITX), and benzoin methyl ether (BME)) will be proposed and the relative improvement observed in FRP or FRPCP discussed.

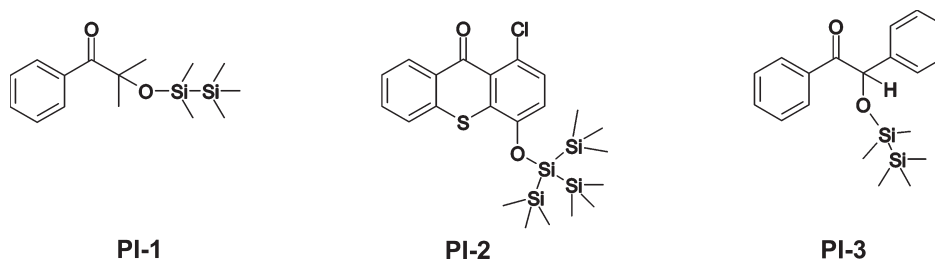
Experimental Section and Computational Procedure

Samples. The new photoinitiators are presented in Scheme 1. 2,2'-Dimethoxyphenylacetophenone (DMPA) used as a reference photoinitiator (Irgacure 651 from Ciba or KB-1 from Lamberti-Spa), benzoin methyl ether (BME), 2,2,6,6-tetramethylpiperidine-*N*-oxyl (TEMPO), and diphenyliodonium hexafluorophosphate (Ph₂I⁺) were obtained from Aldrich, 2-isopropylthioxanthone (ITX) was from Lamberti-Spa., and 2-hydroxy-2-methyl-1-phenylpropanone (HMPP) (Irgacure 1173) was from Ciba (Basel). 1-Chloro-4-hydroxythioxanthone was obtained from Dr. A. Green, Great Lakes Fine Chemicals Ltd., and 1-chloro-4-propoxythioxanthone was a gift from Dr. D. Anderson.

Synthetic Procedure for PI-1, PI-2, and PI-3. 2-Methyl-2-(1,1,2,2,2-pentamethyldisilyloxy)-1-phenylpropan-1-one (**PI-1**). HMPP (563 μL, 3.77 mmol) and pentamethyldisilane (693 μL,

*Corresponding author. E-mail: j.lalevee@uha.fr.

Scheme 1



3.77 mmol, 1 equiv) were added at 0 °C dropwise over 10 min to a solution of tris(pentafluorophenyl)borane (77 mg, 0.15 mmol, 0.04 equiv) in dichloromethane (4 mL). After being stirred at room temperature for 3 h, the reaction mixture was concentrated under reduced pressure, and the crude product was purified by silica gel chromatography (cyclohexane/ethyl acetate 100:1 to 100:2) to give **PI-1** (220 mg, 0.75 mmol, 20%). RMN ^1H (CDCl_3 , 300 MHz): δ 8.17 (dd, $J = 1.1, 8.3$ Hz, 2H), 7.5 (m, 1H), 7.42–7.37 (2H), 1.57 (s, 6H), 0.15 (s, 6H), 0.01 (s, 9H). RMN ^{13}C (CDCl_3 , 75 MHz): δ 203.7, 135.0, 132.2, 130.4, 127.8, 80.8, 29.1, 1.6, –2.3.

1-Chloro-4-(1,1,1,3,3,3-hexamethyl-2-(trimethylsilyl)trioxo-2-yl-oxy)-9H-thioxanthene-9-one (PI-2). A solution of tris(trimethylsilyl)silane (0.93 mL, 3 mmol) in carbon tetrachloride (15 mL) was stirred at room temperature for 12 h. The solvent was evaporated, leaving the corresponding tris(trimethylsilyl)chloride. Then, potassium bis(trimethylsilyl)amide (3.45 mL, 2.3 mmol, 15% in toluene, 1.1 equiv) was added at 0 °C to a solution of 1-chloro-4-hydroxythioxanthone (550 mg, 2.1 mmol) in THF (15 mL). The reaction mixture was stirred at 0 °C for 15 min, and tris(trimethylsilyl)chloride (3 mmol, 1.4 equiv) in THF (3 mL) was added. After being stirred at room temperature for 2 h, the reaction mixture was diluted with water, extracted with ethyl acetate, washed with brine, dried over magnesium sulfate, filtered, and concentrated under reduced pressure. The crude product was purified by silica gel chromatography (cyclohexane/ethyl acetate 20:1) to give **PI-2** (10 mg, 0.2 mmol, 1%). This product being quite unstable, the polymerization, LFP, and ESR experiments were carried out on fresh samples. RMN ^1H (CDCl_3 , 300 MHz): δ 8.46 (d, $J = 9.3$ Hz), 7.59–7.57 (2H), 7.46 (ddd, $J = 2.8, 5.4, 8.1$, 1H), 7.38 (d, $J = 8.5$ Hz, 1H), 6.94 (d, $J = 8.5$ Hz, 1H), 0.27 (s, 18 H), 0.19–0.15 (9H). RMN ^{13}C (CDCl_3 , 75 MHz): δ 180.5, 152.4, 135.8, 132.7, 131.9, 130.9, 129.7, 129.1, 127.3, 126.6, 126.5, 126.1, 118.2, 0.3, –0.7.

2-(1,1,2,2,2-Pentamethyldisilyloxy)-1,2-diphenylethanone (PI-3). Chloropentamethyldisilane (410 μL , 2.1 mmol, 1.5 equiv), imidazole (192 mg, 2.82 mmol, 2 equiv), and DMAP (35 mg, 0.287 mmol, 0.2 equiv) were added at room temperature to a solution of benzoin (300 mg, 1.41 mmol) in DMF (3.5 mL). After being stirred at room temperature for 18 h, the reaction mixture was diluted with water, extracted with cyclohexane/dichloromethane (90/10), washed with brine, dried over magnesium sulfate, filtered, and concentrated under reduced pressure. The crude product was purified by silica gel chromatography (cyclohexane/ethyl acetate 100:1) to give **PI-3** (200 mg, 0.58 mmol, 41%). RMN ^1H (CDCl_3 , 300 MHz): δ 8.01 (dd, $J = 1.2, 8.3$ Hz, 2H), 7.48 (dd, $J = 7.5, 11.6$ Hz, 4H), 7.35 (dd, $J = 7.6, 11.6$ Hz, 4H), 5.72 (s, 1H), 0.22 (s, 3H), 0.19 (s, 3H), 0.04 (s, 9H). RMN ^{13}C (CDCl_3 , 75 MHz): δ 198.9, 134.4, 132.8, 129.8, 128.5 (2 \times C), 128.1 (2 \times C), 127.7, 125.9 (2 \times C), 80.5, –0.47, –0.51, –2.3 (3 \times C).

Polymerization. In film FRP experiments (50 μm thick films), a given photoinitiator (weight concentrations of 1% for **PI-1** to **PI-3** are used in order to get a good solubility) was dissolved in the polymerizable medium (Ebecryl 605 from Cytec). For comparison, DMPA was used in the same conditions. The polymerization conditions have been described in detail in ref 12 (polychromatic light of a Xe–Hg lamp (Hamamatsu, L8252, 150 W)). The evolution of the double-bond content was continuously followed by real-time FTIR spectroscopy (Nexus 870,

Nicolet) as described in ref 12. The rates of polymerization R_p were calculated from the early times of the conversion vs time curves (this part, 0–15% of conversion, being linear for the PIs investigated). In FRPCP experiments, weight concentrations of 1% in diphenyliodonium hexafluorophosphate (Ph_2I^+ from Aldrich) and 1% in PI were used to polymerize a di(cycloaliphatic epoxide) monomer (Cyracure 6110 from Dow). To investigate the photosensitization ability of Ph_2I^+ by PI, a cutoff filter has been used to select $\lambda > 300$ nm (polychromatic light delivered by a Xe–Hg lamp: Hamamatsu, L8252, 150 W). The evolution of the epoxy group content is continuously followed by real-time FTIR spectroscopy; the absorbance of the epoxy group was monitored at about 800 cm^{-1} .¹³

Computational Procedure. Molecular orbital calculations were carried out with the Gaussian 03 suite of programs;¹⁴ the different triplet energy levels (E_T) and the bond dissociation energies (BDE) were calculated at the UB3LYP/6-31G* level. The different optimized geometries were frequency checked.

Laser Flash Photolysis. Nanosecond laser flash photolysis (LFP) experiments were carried out using a Q-switched nanosecond Nd:YAG laser ($\lambda_{\text{exc}} = 355$ nm, 9 ns fwhm pulses; energy reduced down to 10 mJ) from Continuum (Powerlite 9010) and an analyzing system consisting of a pulsed xenon lamp, a monochromator, a fast photomultiplier, and a transient digitizer.¹⁵

ESR Spin-Trapping Experiments. ESR spin-trapping experiments (a now recognized powerful technique for the identification of the radical center)¹⁶ were carried out using a X-band spectrometer (MS 200 Magnetech). The radicals generated under the light irradiation (Xe–Hg lamp (Hamamatsu, L8252, 150 W; $\lambda > 310$ nm)) were trapped by phenyl-*N-tert*-butylnitron (PBN), 5,5-dimethyl-1-pyrroline *N*-oxide (DMPO), or 3,3,5,5-tetramethylpyrroline *N*-oxide (4MPO). The ESR spectra simulations were carried out with the PEST WINSIM program.¹⁷

Results and Discussion

a. Absorption Properties. The UV absorption properties of **PI-1**–**PI-3** are depicted in Figure 1. For **PI-1**, the absorption maximum is slightly shifted compared to the unsubstituted compound HMPP, i.e., 328 nm instead of 317 nm in acetonitrile. For **PI-2**, the absorption is typical of the thioxanthone chromophore and exhibits an absorption maximum at 386 nm in acetonitrile. For **PI-3**, a slight hyperchromic effect is noted compared to benzoin methyl ether BME.

b. Free Radical Photopolymerization FRP Ability. The proposed photoinitiators are liquid (compared for example to BME or TX which are solid), a property useful to improve the solubility in viscous acrylate matrix for practical applications.

The photoinitiating abilities of **PI-1** to **PI-3** in FRP were investigated and compared to that of the well-known type I photoinitiator DMPA (Figure 2). The relative polymerization rates are given in Table 1. **PI-1** and **PI-3** can be considered as powerful photoinitiators as the efficiencies are similar to that of DMPA.

Compared to HMPP, **PI-1** exhibits a slightly reduced ability in laminated conditions. In aerated media, however,

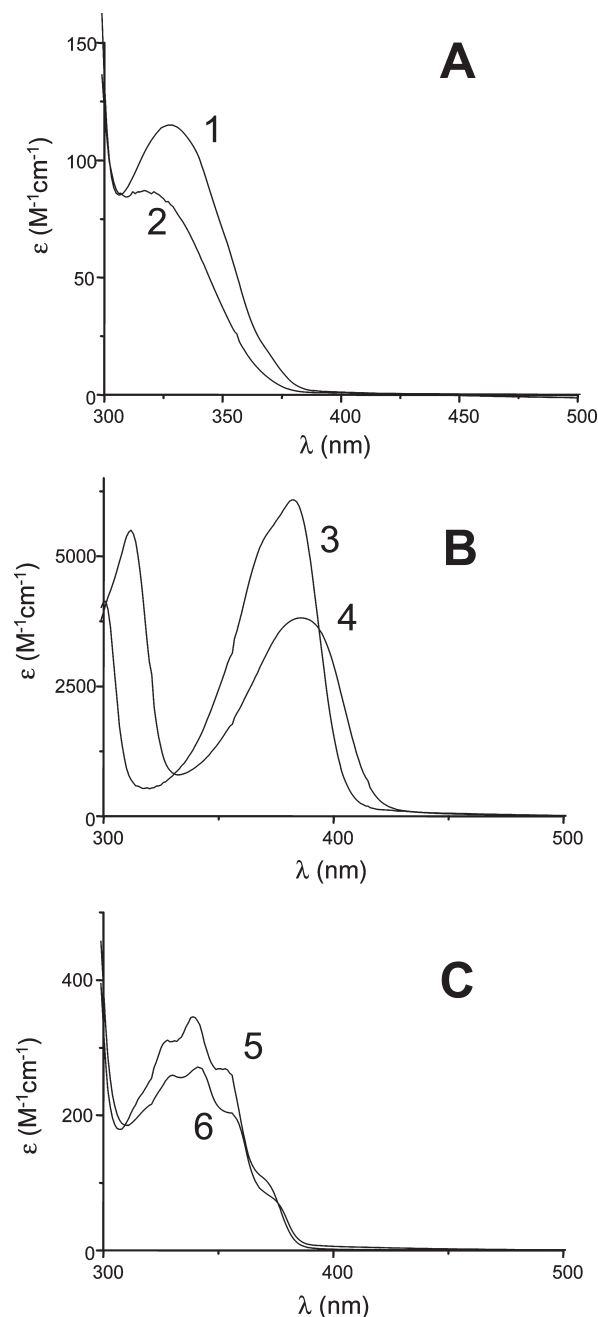


Figure 1. UV absorption properties: (A) **PI-1** (1) compared to HMPP (2). (B) ITX (3) and **PI-2** (4) in acetonitrile. (C) **PI-3** (5) and BME (6) in *tert*-butylbenzene.

it shows a slightly reduced oxygen inhibition. This should be in line with the known ability of silyl radicals to overcome the detrimental effect of oxygen as evidenced in.⁸ **PI-2** is a much better photoinitiating system than ITX alone (Figure 2B). For 1-chloro-4-hydroxythioxanthone and 1-chloro-4-propoxythioxanthone, the polymerization rates were found quite similar to ITX (reactivity ratio 0.9 and 1.5, respectively). This also demonstrates that the silyl substitution in **PI-2** increases the polymerization ability.

When using ITX, the initiating radicals are generated by a hydrogen abstraction reaction with the monomer. This thioxanthone derivative based compound (**PI-2**) behaves as a type I photoinitiating system but remains less efficient than DMPA in term of R_p (the limit % conversion is however almost the same). Of course, the addition of an amine also

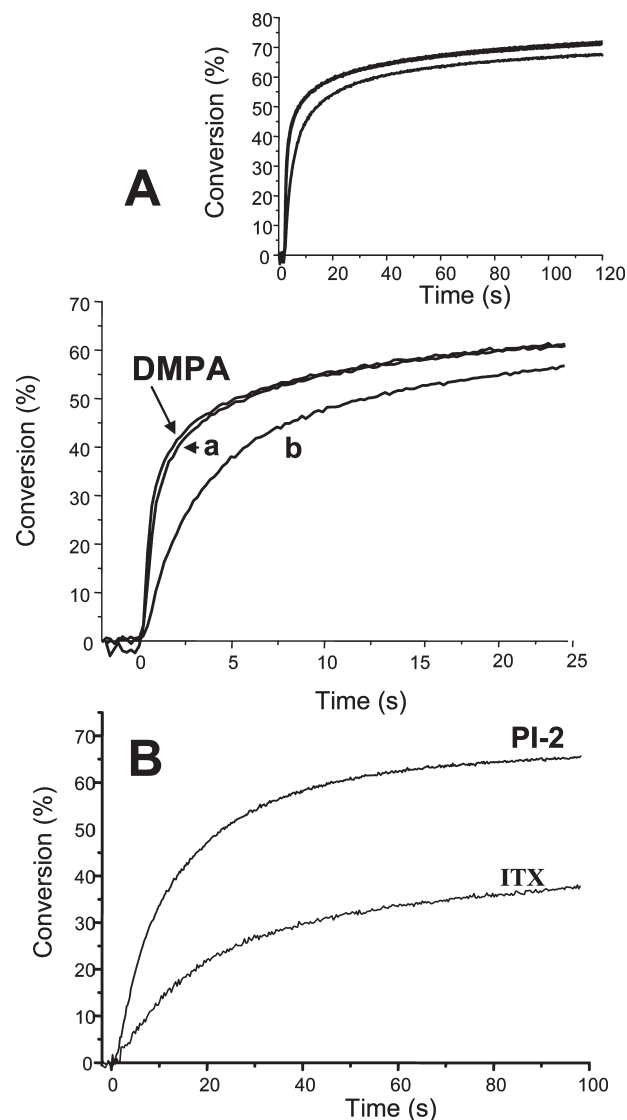


Figure 2. (A) Radical photopolymerization ability of (a) **PI-1** and (b) **PI-2** as photoinitiators compared to DMPA (1% w/w) in an Ebecryl 605 film (laminated conditions). (B) Radical photopolymerization ability of **PI-2** as photoinitiators compared to ITX (1% w/w) in an Ebecryl 605 film (laminated conditions; a different light intensity than for (A) is used). For 1-chloro-4-hydroxythioxanthone and 1-chloro-4-propoxythioxanthone, the relative reactivity (polymerization rates) compared to ITX is 0.9 and 1.5, respectively.

Table 1. Radical Polymerization Ability of the Different PIs Expressed as $R_p/[M_0]$ (s^{-1})^a

| | $R_p/[M_0] \times 100$ | |
|-------------|---------------------------|---------------------------|
| | laminated | air |
| DMPA | 67 | 55 |
| PI-1 | 46 (55 ^b) | 43 (40 ^b) |
| PI-2 | 15 (45.7 ^c) | 7.3 (22.3 ^c) |
| PI-3 | 40.7 (30.1 ^d) | 37.6 (28.9 ^d) |

^a $[M_0]$ is the initial monomer concentration. $[PI] = 1\%$ w/w. ^b For HMPP. ^c In the presence of triethylamine 1% w/w. ^d For BME.

improves the R_p s: **PI-2** can also work in type II systems. **PI-3** is characterized by a higher efficiency than BME (in both laminated and aerated conditions). This is in contrast to the results obtained with benzoin trimethylsilyl ether for the methyl methacrylate polymerization (see below).^{5a}

c. Free Radical Promoted Cationic Photopolymerization FRPCP Ability. Figure 3 shows the relative efficiency

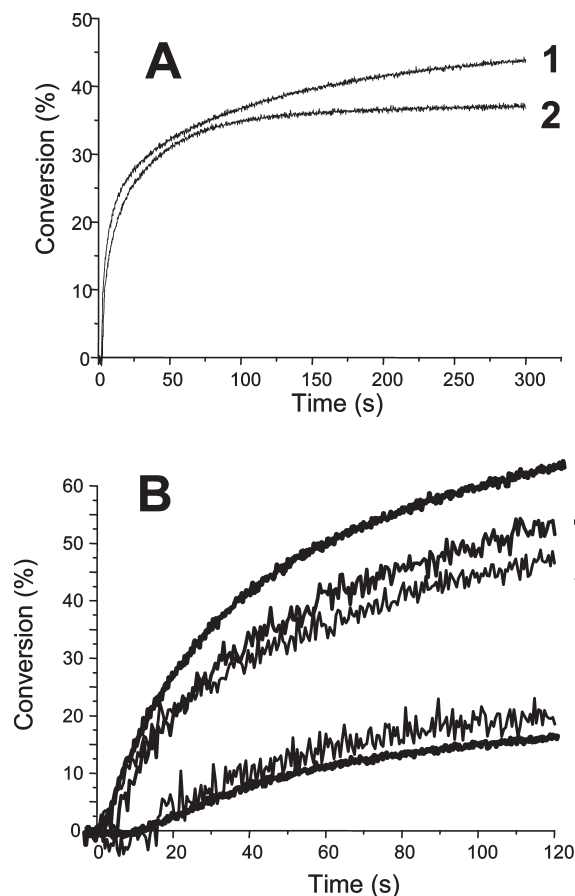


Figure 3. Cationic photopolymerization of Cyracure 6110 under air: (A) in the presence of (1) ITX/ Ph_2I^+ and (2) **PI-2**/ Ph_2I^+ ; (B) in the presence of (3) **PI-3**/ Ph_2I^+ , (4) **PI-1**/ Ph_2I^+ , (5) DMPA/ Ph_2I^+ , (6) HMPP/ Ph_2I^+ , and (7) BME/ Ph_2I^+ . Photoinitiator/ Ph_2I^+ : 1%/1% w/w.

of **PI-1**/ Ph_2I^+ , **PI-2**/ Ph_2I^+ , and **PI-3**/ Ph_2I^+ as cationic photo-initiating systems (compared to the well-known reference DMPA/ Ph_2I^+) in aerated conditions. As arylidonium salts show a main absorption band at $\lambda < 300$ nm, the initiation ability of Ph_2I^+ alone in our irradiation conditions ($\lambda > 300$ nm) is fairly low. Using **PI-1** to **PI-3** leads to a dramatic increase of both the R_p and the final conversion. The efficiencies of **PI-2**/ Ph_2I^+ and ITX/ Ph_2I^+ are similar (Figure 3A). For **PI-1** (or **PI-3**), remarkable improvements compared to HMPP/ Ph_2I^+ (or BME/ Ph_2I^+) are observed (Figure 3B). Interestingly both the **PI-1**/ Ph_2I^+ and **PI-3**/ Ph_2I^+ combinations are more efficient than DMPA/ Ph_2I^+ (this system is rather efficient as the oxidation of the phenyldimethoxybenzyl radical by the iodonium salts is assumed to readily occur, leading to a cation which initiates the polymerization process). The best result is obtained for **PI-3**.

d. Potentially Cleavable Bonds. The calculated bond dissociation energies (BDE) associated with the different potential cleavage processes are indicated by arrows in Scheme 2. Several bonds requiring an energy around 230–282 kJ/mol can be broken.

e. Radicals Observed by the ESR Spin-Trapping Technique. Under direct irradiation, the benzoyl radical is observed ($g \sim 2.0008$, $a_{2\text{H}} = 1.2$ G) for **PI-1** and **PI-3** (Figure 4).^{16d} However, for a better characterization of the photochemical processes on PI, the spin-trapping technique has been used.^{16d}

Different radicals are generated upon light irradiation and trapped with PBN, DMPO, or 4MPO (Figure 4; **PI-1**–**PI-3**). The hyperfine splittings (hfs constants) of these adducts for

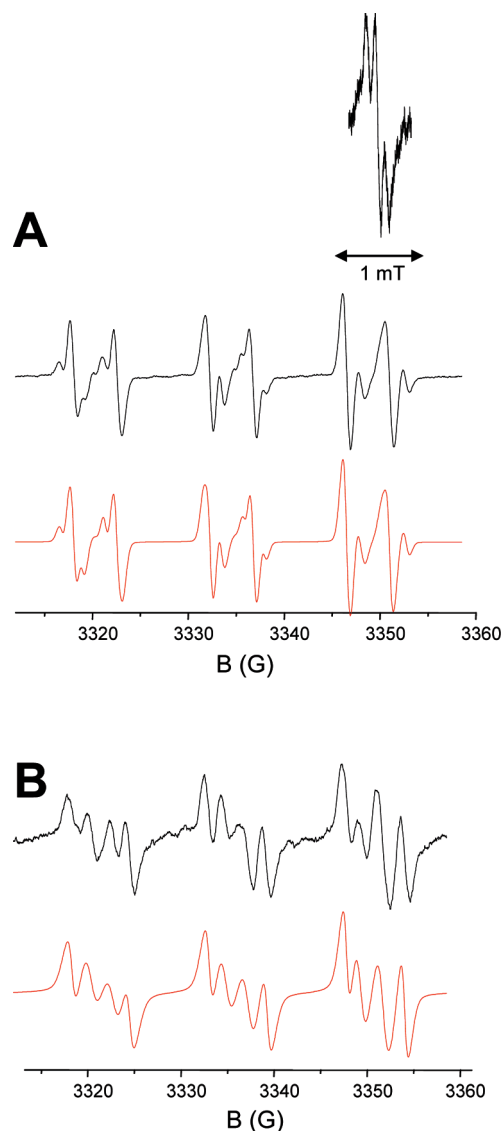
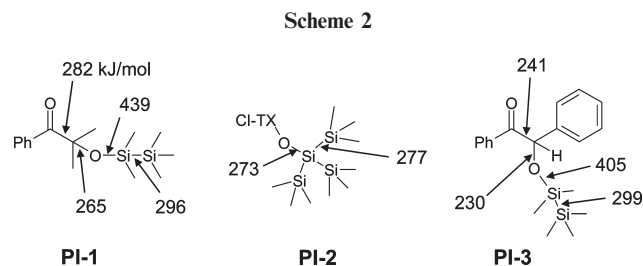


Figure 4. ESR spin-trapping experiments under the UV light irradiation of **PI-1** or **PI-2** (0.01 M) at $\lambda > 300$ nm: experimental (top) and simulated (bottom) spectra (see text): (A) **PI-1**/PBN; (B) **PI-2**/PBN. Inset: the benzoyl radical observed under irradiation of **PI-3** without spin trap ($g = 2.0008$; $a_{\text{H}} = 0.12$ mT).



both the nitrogen (a_{N}) and the hydrogen (a_{H}) are reported in Table 2. Schemes 3–5 show the possible routes for the generation of these radicals.

In **PI-1**, radicals generated by a α -cleavage process are observed (reaction 1 in Scheme 3): a benzoyl radical (**a**) ($a_{\text{N}} = 14.3$; $a_{\text{H}} = 4.5$ G for PBN) and an α -oxyalkyl radical (**b**) ($a_{\text{N}} = 14.4$; $a_{\text{H}} = 24.5$ G for DMPO). A β -cleavage process is also noted (reaction 2 in Scheme 3) as evidenced by the observation of an α -carbonylalkyl radical (**c**) ($a_{\text{N}} = 13.6$; $a_{\text{H}} = 13.2$ G for DMPO) and a silyl radical ($a_{\text{N}} = 14.8$; $a_{\text{H}} = 6.2$ G for PBN).

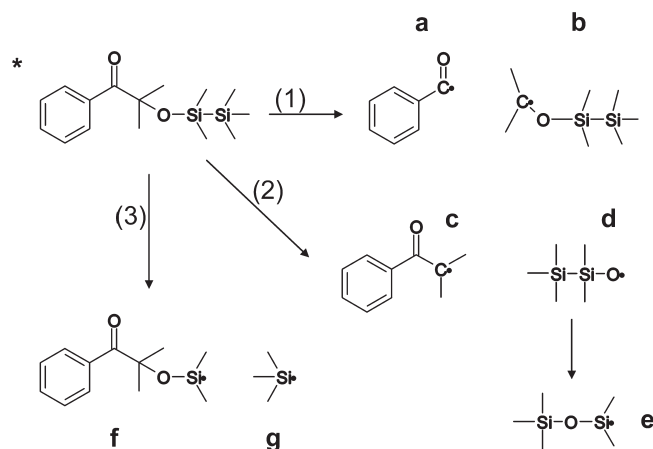
4MPO was used to confirm this Si[•] production (Table 2).^{21b} The formation of silyl radicals (**f** and **g**) through a cleavage of the Si–Si bond (reaction 3 in Scheme 3) can be probably ruled out (see below). The silyl radical is assigned to (**e**). Radical **d** is not observed because of its rearrangement (see below in section f).

Table 2. Hfs Constants of the Radical Adducts Observed in the ESR Spin-Trapping Experiments for PI-1–PI-3 (Proposed Attribution Given in Parentheses)^a

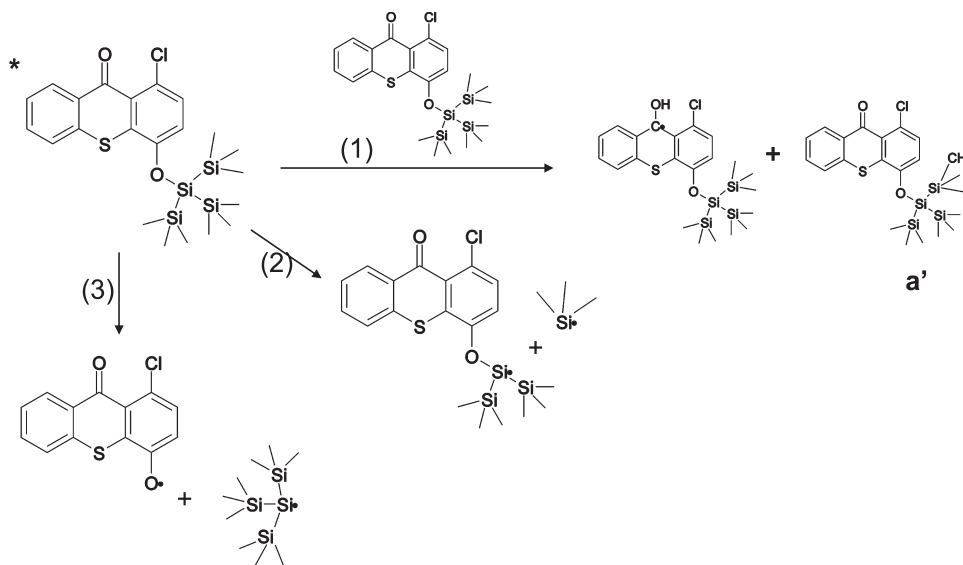
| | | $a_N; a_H$ (G) |
|------|------|---|
| PI-1 | PBN | 14.4, 2.5 (c or b) ^b |
| | | 14.3, 4.5 (a) ^{b,1} |
| | | 14.8, 6.2 (silyl radical) ^{b,2} |
| | DMPO | 14.4, 24.5 (b) ^{b,3} |
| PI-2 | PBN | 13.6, 13.2 (c) ^{b,4} |
| | | 14.6, 29.0 (silyl radical) ^{b,c} |
| | | 14.8, 6.2 (silyl radical) ^{b,2} |
| | DMPO | 14.5, 2.3 (a') ^{b,5} |
| PI-3 | PBN | n.d. |
| | | 14.2, 4.5 (a) ^{b,1} |
| | | 14.8, 6.2 (silyl radical) ^{b,2} |
| | DMPO | n.d. |

^a n.d. = not determined. ^b See text and Schemes 3–5. The attributions are in agreement with the literature data: 1,¹⁸ 2,²¹ 3,¹⁹ 4,²⁰ 5.²¹ ^c For the triethylsilyl radical, the following parameters were obtained: $a_N = 15$, $a_H = 29$ G (this work); this is in excellent agreement with ref 21b.

Scheme 3



Scheme 4



All the assignments are in agreement with those reported for similar radicals.^{18–21}

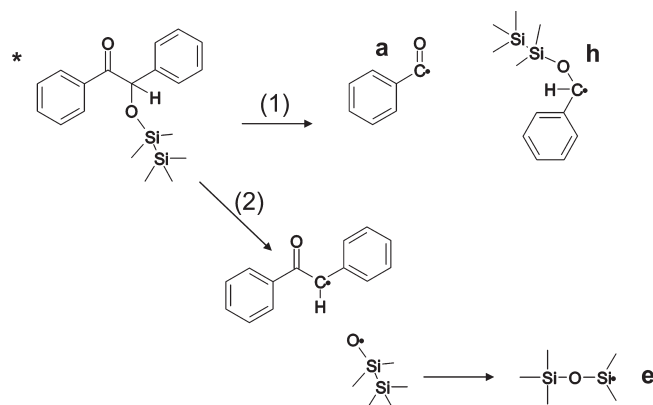
In **PI-2**, both silyl and carbon-centered radicals were observed (Table 2). Such a behavior has been recently observed for 4-tris(trimethylsilyl)silyloxybenzophenone.^{6c} The carbon structure can be ascribed to a silylalkyl radical (**a'**) whose hfs constants are in excellent agreement with the values reported for the known $(CH_3)_3Si-CH_2^{\bullet}$ radical ($a_N = 14.4$ G and $a_H = 2.7$ G using PBN).²¹ The **a'** radical is formed by a hydrogen abstraction reaction between the **PI-2** triplet state and a ground state **PI-2** molecule (reaction 1 in Scheme 4). The hfs constants for the trapped Si[•] are more consistent with a trialkylsilyl radical generated by a Si–Si bond cleavage (reaction 2 in Scheme 4) rather than a tris(trimethylsilyl)silyl radical (whose hfs constants are known)^{6c,21} arising from a O–Si bond cleavage (reaction 3 in Scheme 4).

In **PI-3**, the benzoyl radicals generated by the α -cleavage process are observed (reaction 1 in Scheme 5). Silyl radicals are also clearly found in agreement with a β -cleavage process associated with a rearrangement of the silyloxyl radicals. The benzyl derived radicals (generated from α - and β -cleavages) are not trapped with PBN.

f. Excited-State Processes As Revealed by LFP. The laser excitation of **PI-2** at 355 nm leads to the transient species (Figure 5) with an absorption maximum close to 650 nm that can be ascribed to the triplet state localized on the thioxanthone moiety. The triplet state lifetime ($\sim 5 \mu s$) is much longer than that found for the 4-tris(trimethylsilyl)silyloxybenzophenone^{6c} supporting a lower dissociation rate constant for **PI-2** ($k < 2 \times 10^5 s^{-1}$). This transient is quenched by triethylamine and oxygen with high rate constants (5.5×10^8 and $3.4 \times 10^9 M^{-1} s^{-1}$, respectively). The self-quenching process **³PI-2/PI-2** cannot be investigated due to the intense ground-state absorption of **PI-2** at 355 nm.

The transient species (Figure 5) observed upon laser excitation of **PI-1** at 355 nm is ascribed to the benzoyl radical already known.²² The buildup occurs within the resolution time of our experimental setup (< 10 ns), demonstrating a fast cleavage process. The interaction rate constants with TEMPO and O_2 are very high and also in agreement with this radical structure, i.e., $5.5 \times 10^8 M^{-1} s^{-1}$ and $2.3 \times 10^9 M^{-1} s^{-1}$, respectively.²³ These LFP results are in agreement with the ESR-ST experiments.

Scheme 5



For **PI-3**, the observed species (Figure 5) is characterized by a maximum absorption at about 300 nm and is quenched by TEMPO with a rate constant of $6.3 \times 10^7 \text{ M}^{-1} \text{ s}^{-1}$. It can be ascribed to the silyloxybenzyl radical (**h** in Scheme 5). The benzoyl radical is not detectable in the spectrum because of its low extinction coefficients in the investigated wavelength range as observed previously when exciting BME.²⁸

g. Energetic Considerations. The triplet energy levels E_T of **PI-1** and **PI-3** are calculated as 271 and 277 kJ/mol, respectively (at UB3LYP/6-31G*). The BDE associated with the different cleavage processes are gathered in Scheme 2. Interestingly for both compounds, the β -cleavage is more favorable than the α -cleavage by about 17 kJ/mol for **PI-1** and 11 kJ/mol for **PI-3**. The **d** \rightarrow **e** rearrangement (Scheme 3) is energetically extremely favorable with a reaction exothermicity of -173 kJ/mol (at the UB3LYP/6-31G* level). Such a process has been recently observed for other silyloxyl structures.²⁶ This can probably confirm the observation of the silyl radical (**e**) in ESR spin-trapping as well as the high abilities of **PI-1** and **PI-3** in FRPCP related to the easy oxidation of the silyl radicals.

In polysilanes, it has been previously found that the Si–Si bond cleavage can occur after energy transfer.²⁷ In the present case, this process can be ruled out for the silyl radicals formation in **PI-1** (reaction 3 in Scheme 3). Indeed, the spectroscopic triplet state associated with a Si–Si bond is calculated as 6.1 eV for $(\text{CH}_3)_3\text{Si}-\text{Si}(\text{CH}_3)_3$ as a model compound (at the MPW1PW91/6-31G* level); since $E_T = 2.8 \text{ eV}$ for the acetophenone moiety, an intramolecular triplet–triplet energy transfer to the Si–Si bond is probably highly endergonic and can perhaps explain the absence of **f** and **g**. A similar behavior can be expected for **PI-3**.

The **PI-2** triplet energy (258 kJ/mol) is lower than the BDE(Si–Si) and BDE(O–Si) in agreement with the measured low dissociation rate constant. For 4-tris(trimethylsilyl)silyloxybenzophenone,^{6c} an opposite situation was observed ($E_T > \text{BDE}(\text{Si}-\text{Si})$), leading to a faster cleavage process.

h. Initiation Efficiency. The excellent ability of **PI-1** and **PI-3** is partly ascribed to the formation of silyl radicals under light irradiation; i.e., these species efficiently add to acrylate double bonds in FRP and are easily oxidized by Ph_2I^+ to initiate FRPCP as recently evidenced for other systems.^{6c,f,8} The **PI-1**/HMPP, **PI-2**/ITX, and **PI-3**/BME differences well demonstrate that the initiation mechanisms are different between the starting molecules and the silylated structures.

For **PI-1** and **PI-3**, reactions 1 and 2 appear as the major deactivation pathways. The relative ratio of β - vs α -cleavage can hardly be determined. Only benzoyl (for **PI-1**) or benzyl (for **PI-3**) derived radicals significantly

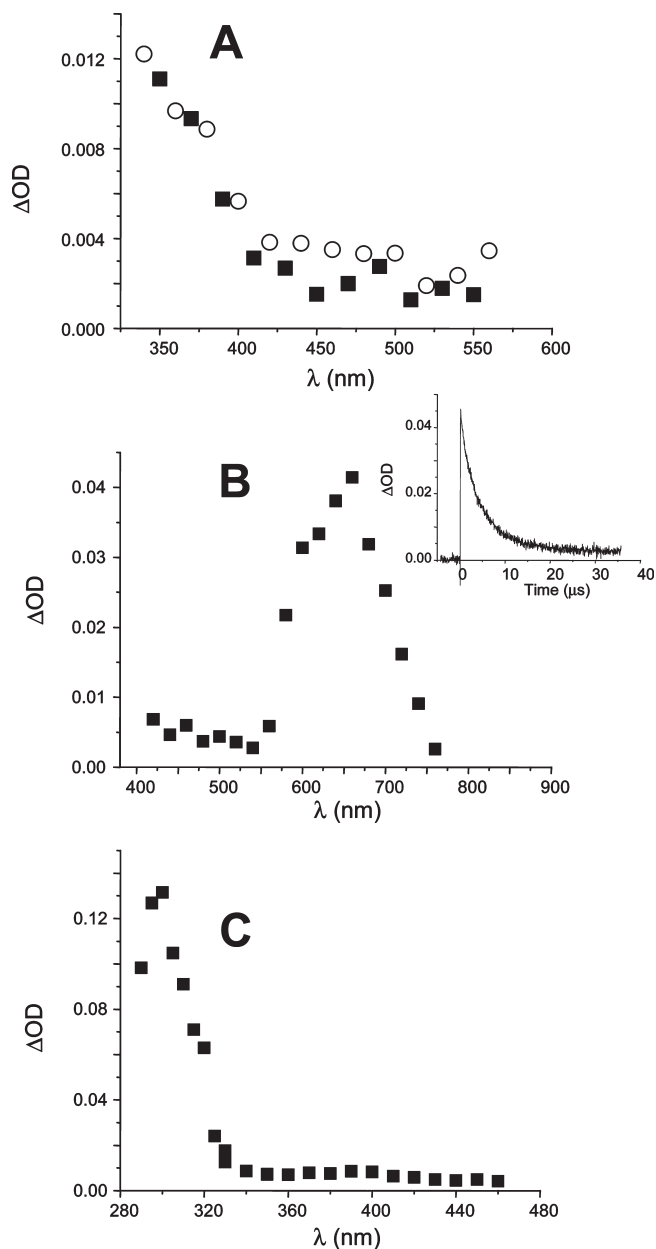


Figure 5. Transient spectra observed after laser excitation at 355 nm of (A) **PI-1** (circle) and HMPP (square), (B) **PI-2**, and (C) **PI-3**. Solvent: acetonitrile; recording time: $t = 0 \text{ } \mu\text{s}$.

absorb in LFP (silyl or α -carbonylalkyl radicals weakly absorb at $\lambda > 330 \text{ nm}$).^{24,28} The ESR spin-trapping does not allow an access to this ratio since the selectivity of the different generated radicals toward the addition to PBN or DMPO can be different.²⁵ However, for different spin-trap concentrations, the adducts formed from α - and β -cleavages are present in high yields, probably demonstrating that both pathways are important.

In **PI-1**, the **d** to **e** rearrangement is probably decisive (reaction 2 in Scheme 3) for the production of efficient silyl radicals. In **PI-2**, the hydrogen abstraction and the Si–Si bond dissociation (reactions 1 and 2 in Scheme 4) are the major pathways for the radical formation. As a consequence, the thioxanthone derivative **PI-2** also behaves as a type I PI. These processes are in agreement with the better ability of this compound compared to ITX in FRP. The high efficiency of **PI-3** (particularly for FRPCP) is ascribed to the generation of silyl radicals through the rearrangement of silyloxyl

radicals after the β -cleavage (reaction 2 in Scheme 5). Such a process in the absence of a Si–Si bond (like for the benzoin trimethylsilyl ether)^{5a} can obviously not occur, thereby preventing the silyl radicals formation. This can probably demonstrate that the introduction of a O–Si–Si fragment is requested.

Conclusion

In the present paper, new efficient silyl moiety containing photoinitiators both for FRP and FRPCP processes are proposed. Their polymerization ability in silicone–acrylate matrix where a good photoinitiator solubility is requested will be investigated in forthcoming works as well as the development of new structures. Preliminary calculations suggest that the Si containing moiety could be advantageously changed for a Ge-based group. The rather hard synthesis of new Ge-containing conventional PI is under way.

Acknowledgment. The authors thank Dr. A. Green, Great Lakes Fine Chemicals Ltd., for the gift of 1-chloro-4-hydroxythioxanthone and Dr. D. Anderson for the 1-chloro-4-propoxythioxanthone sample (CPTX).

Supporting Information Available: NMR spectra for PI-1, PI-2, and PI-3. This material is available free of charge via the Internet at <http://pubs.acs.org>.

References and Notes

- (1) (a) Dietliker, K. *A Compilation of Photoinitiators Commercially Available for UV Today*; Sita Technology Ltd.: Edinburgh, London, 2002. (b) Neckers, D. C. *UV and EB at the Millenium*; Sita Technology: London, 1999. (c) *Photoinitiated Polymerization*; Belfied K. D., Crivello, J. V., Eds.; ACS Symposium Series 847; American Chemical Society: Washington, DC, 2003. (d) Fouassier, J. P. *Photoinitiation, Photopolymerization and Photocuring: Fundamental and Applications*; Hanser Publishers: New York, 1995. (e) *Photochemistry and UV Curing*; Fouassier, J. P., Ed.; Researchsignpost: Trivandrum, India, 2006.
- (2) (a) Liska, R.; Knaus, S.; Gruber, H.; Wendrinsky, J. *Surf. Coat. Int.* **2000**, *83*, 297–303. (b) Liska, R. *J. Polym. Sci., Part A: Polym. Chem.* **2002**, *40*, 1504–1518. (c) Liska, R.; Herzog, D. *J. Polym. Sci., Part A: Polym. Chem.* **2004**, *42*, 752–764. (d) Liska, R.; Seidl, B. *J. Polym. Sci., Part A: Polym. Chem.* **2005**, *43*, 101–111. (e) Ullrich, G.; Ganster, B.; Salz, U.; Moszner, N.; Liska, R. *J. Polym. Sci., Part A: Polym. Chem.* **2006**, *44*, 1686–1700. (f) Seidl, B.; Kalinyaprak-Icten, K.; Fuss, N.; Hofer, M.; Liska, R. *J. Polym. Sci., Part A: Polym. Chem.* **2007**, *46*, 289–301. (g) Seidl, B.; Liska, R.; Grabner, G. *J. Photochem. Photobiol., A* **2006**, *180*, 109–117.
- (3) (a) Catalina, F.; Corrales, T.; Peinado, C.; Allen, N. S.; Green, W.; Timms, A. *Polymer* **1993**, *29*, 125–129. (b) Corrales, T.; Catalina, F.; Allen, N. S.; Peinado, C. In *Photochemistry and UV Curing*; Fouassier, J. P., Ed.; Researchsignpost: Trivandrum, India, 2006; pp 31–44.
- (4) (a) Gacal, B.; Akat, H.; Balta, D. K.; Arsu, N.; Yagci, Y. *Macromolecules* **2008**, *41*, 2401–2405. (b) Degirmenci, M.; Cianga, I.; Yagci, Y. *Macromol. Chem. Phys.* **2002**, *203*, 1279–1284. (c) Degirmenci, M.; Hizal, G.; Yagci, Y. *Macromolecules* **2002**, *35*, 8265–8270. (d) Aydin, M.; Arsu, N.; Yagci, Y.; Jockusch, S.; Turro, N. J. *Macromolecules* **2005**, *38*, 4133–4138. (e) Temel, G.; Arsu, N.; Yagci, Y. *Polym. Bull.* **2006**, *57*, 51–56. (f) Tasdelen, M. A.; Kumbaraci, Y.; Talinli, N.; Yagci, Y. *Polymer* **2006**, *47*, 7611–7614. (g) Balta, D. K.; Arsu, N.; Yagci, Y.; Jockusch, S.; Turro, N. J. *Macromolecules* **2007**, *40*, 4138–4141.
- (5) (a) Woo, H.-G.; Hong, L.-Y.; Kim, S.-Y.; Choi, Y.-K.; Kook, S.-K.; Ham, H.-S. *Bull. Korean Chem. Soc.* **1995**, *16*, 667–670. (b) Dietlin, C.; Allonas, X.; Morlet-Savary, F.; Fouassier, J. P.; Visconti, M.; Norcini, G.; Romagnano, S. *J. Appl. Polym. Sci.* **2008**, *109*, 825–833. (c) Dietlin, C.; Lalevée, J.; Allonas, X.; Fouassier, J. P.; Visconti, M.; Li Bassi, G.; Norcini, G. *J. Appl. Polym. Sci.* **2008**, *107*, 246–252.
- (6) (a) Arsu, N.; Hizal, G.; Yagci, Y. *Macromol. Rep.* **1995**, 1257–1262. (b) Kmínek, I.; Yagci, Y.; Schnabel, W. *Polym. Bull.* **1992**, *29*, 277–282. (c) Peinado, C.; Alonso, A.; Catalina, F.; Schnabel, W. *J. Photochem. Photobiol., A* **2001**, *141*, 85–91. (d) West, R.; Wolff, A. R.; Peterson, D. J. *J. Radiat. Curing* **1986**, *13*, 35–41. (e) Lalevée, J.; Blanchard, N.; El-Roz, M.; Graff, B.; Allonas, X.; Fouassier, J. P. *Macromolecules* **2008**, *41*, 4180–4186. (f) Lalevée, J.; Allonas, X.; Fouassier, J. P. *Chem. Phys. Lett.* **2009**, *469*, 298–303.
- (7) (a) Ganster, B.; Fischer, U. K.; Moszner, N.; Liska, R. *Macromol. Rapid Commun.* **2008**, *29*, 57–62. (b) Ganster, B.; Fischer, U. K.; Moszner, N.; Liska, R. *Macromolecules* **2008**, *41*, 2394–2400. (c) Durmaz, Y. Y.; Moszner, N.; Yagci, Y. *Macromolecules* **2008**, *41*, 6714–6718.
- (8) (a) Lalevée, J.; Allonas, X.; Fouassier, J. P. *J. Org. Chem.* **2007**, *72*, 6434–6439. (b) Lalevée, J.; El-Roz, M.; Allonas, X.; Fouassier, J. P. *Macromolecules* **2007**, *40*, 8527–8530. (c) Lalevée, J.; Dirani, A.; El-Roz, M.; Allonas, X.; Fouassier, J. P. *Macromolecules* **2008**, *41*, 2003–2010. (d) Lalevée, J.; El-Roz, M.; Allonas, X.; Fouassier, J. P. *J. Polym. Sci., Part A: Chem.* **2008**, *46*, 2008–2014.
- (9) Lalevée, J.; Dirani, A.; El-Roz, M.; Allonas, X.; Fouassier, J. P. *J. Polym. Sci., Part A: Chem.* **2008**, *46*, 3042–3047.
- (10) Lalevée, J.; Tehfe, M. A.; Allonas, X.; Fouassier, J. P. *Macromolecules* **2008**, *41*, 9057–9062.
- (11) (a) Kolar, A.; Gruber, H. F.; Greber, G. *J. Macromol. Sci., Pure Appl. Chem.* **1994**, *A31* (3), 305–318. (b) Baudin, G.; Jung, T. US Patent Number 7,105,582 B2, 2006.
- (12) (a) Lalevée, J.; Allonas, X.; Jrad, S.; Fouassier, J. P. *Macromolecules* **2006**, *39*, 1872–1879. (b) Lalevée, J.; Zadoina, L.; Allonas, X.; Fouassier, J. P. *J. Polym. Sci., Part A: Chem.* **2007**, *45*, 2494–2502.
- (13) El-Roz, M.; Lalevée, J.; Morlet-Savary, F.; Allonas, X.; Fouassier, J. P. *J. Polym. Sci., Part A: Chem.* **2008**, *46*, 7369–7375.
- (14) (a) Gaussian 03, Revision B.2; Frisch, M. J.; Trucks, G. W.; Schlegel, H. B.; Scuseria, G. E.; Robb, M. A.; Cheeseman, J. R.; Zakrzewski, V. G.; Montgomery, J. A., Jr.; Stratmann, R. E.; Burant, J. C.; Dapprich, S.; Millam, J. M.; Daniels, A. D.; Kudin, K. N.; Strain, M. C.; Farkas, O.; Tomasi, J.; Barone, V.; Cossi, M.; Cammi, R.; Mennucci, B.; Pomelli, C.; Adamo, C.; Clifford, S.; Ochterski, J.; Petersson, G. A.; Ayala, P. Y.; Cui, Q.; Morokuma, K.; Salvador, P.; Dannenberg, J. J.; Malick, D. K.; Rabuck, A. D.; Raghavachari, K.; Foresman, J. B.; Cioslowski, J.; Ortiz, J. V.; Baboul, A. G.; Stefanov, B. B.; Liu, G.; Liashenko, A.; Piskorz, P.; Komaromi, I.; Gomperts, R.; Martin, R. L.; Fox, D. J.; Keith, T.; Al-Laham, M. A.; Peng, C. Y.; Nanayakkara, A.; Challacombe, M.; Gill, P. M. W.; Johnson, B.; Chen, W.; Wong, M. W.; Andres, J. L.; Gonzalez, C.; M. Head-Gordon, Replogle, E. S.; Pople, J. A. Gaussian, Inc.: Pittsburgh, PA, 2003. (b) Foresman, J. B.; Frisch, A. *Exploring Chemistry with Electronic Structure Methods*, 2nd ed.; Gaussian Inc., 1996.
- (15) Lalevée, J.; Allonas, X.; Fouassier, J. P. *J. Am. Chem. Soc.* **2002**, *124*, 9613–9621.
- (16) (a) Tordo, P. *Spin-Trapping: Recent Developments and Applications*. In Atherton, N. M.; Davies, M. J.; Gilbert, B. C., Eds.; *Electron Spin Resonance*; The Royal Society of Chemistry: Cambridge, 1998; Vol. 16. (b) Chignell, C. F. *Pure Appl. Chem.* **1990**, *62*, 301–308. (c) Kotake, Y.; Kuwata, K. *Bull. Chem. Soc. Jpn.* **1981**, *54*, 394–399. (d) Alberti, A.; Benaglia, M.; Macciantelli, D.; Rossetti, S.; Scoponi, M. *Eur. Polym. J.* **2008**, *44*, 3022–3027.
- (17) Duling, D. R. *J. Magn. Reson., Ser. B* **1994**, *104*, 105–112.
- (18) Baumann, H.; Timpe, H. J.; Zubarev, V. E.; Fok, N. V.; Mel'nikov, M. V. *J. Photochem.* **1985**, *30*, 487–500.
- (19) Janzen, E. G.; Liu, J.-P. *J. Magn. Reson.* **1973**, *9*, 510–512.
- (20) Yarkov, S. P.; Belevskii, V. N.; Zubarev, V. E. *Khim. Vys. Energ.* **1980**, *14*, 115–120.
- (21) (a) Chandra, H.; Davidson, I. M. T.; Symons, M. C. R. *J. Chem. Soc., Faraday Trans. 1* **1983**, *79*, 2705–2711. (b) Alberti, A.; Leardini, R.; Pedullì, G. F.; Tundo, A.; Zanardi, G. *Gazz. Chim. Ital.* **1983**, *113*, 869–871.
- (22) Fouassier, J. P.; Lougnot, D. J.; Scaiano, J. C. *Chem. Phys. Lett.* **1989**, *160*, 335–339.
- (23) Brown, C. E.; Neville, A. G.; Rayner, D. M.; Ingold, K. U.; Luszyk, J. *Aust. J. Chem.* **1995**, *48*, 363–379.
- (24) Chatgililoglu, C. In *Organosilanes in Radical Chemistry*; John Wiley & Sons: New York, 2004.
- (25) Criqui, A.; Lalevée, J.; Allonas, X.; Fouassier, J. P. *Macromol. Chem. Phys.* **2008**, *209*, 2223–2231.
- (26) Zaborovskiy, A. B.; Lutsyk, D. S.; Prystansky, R. E.; Kopylets, V. I.; Timokhin, V. I.; Chatgililoglu, C. *J. Organomet. Chem.* **2004**, *689*, 2912–2919.
- (27) El-Roz, M.; Lalevée, J.; Morlet-Savary, F.; Allonas, X.; Fouassier, J. P., to be submitted.
- (28) Shrestha, N. K.; Yagi, E. J.; Takatori, Y.; Kawai, A.; Kajii, Y.; Shibuya, K.; Obi, K. *J. Photochem. Photobiol. A* **1998**, *116*, 179–185.